Available online at www.sciencedirect.com
ScienceDirect
Journal of Power Sources 175 (2008) 441–446
JOURNAL OF POWER SOURCES
www.elsevier.com/locate/jpowsour

Short communication

Nonlinear dynamic modeling for a SOFC stack by using a Hammerstein model

Hai-Bo Huo [a,∗], Zhi-Dan Zhong [a,b], Xin-Jian Zhu [a], Heng-Yong Tu [a]

[a] *Fuel Cell Research Institute, Shanghai Jiao Tong University, Shanghai 200240, China*
[b] *College of Electromechanical Engineering, Henan University of Science and Technology, Luoyang 471003, Henan Province, China*

Received 3 July 2007; received in revised form 15 September 2007; accepted 17 September 2007
Available online 26 September 2007

Abstract

Solid oxide fuel cell (SOFC) is a kind of nonlinear, multi-input–multi-output (MIMO) system that is hard to model by the traditional methodologies. For the purpose of dynamic simulation and control, this paper reports a dynamic modeling study of SOFC stack using a Hammerstein model. The static nonlinear part of the Hammerstein model is modeled by a radial basis function neural network (RBFNN), and the linear part is modeled by an autoregressive with exogenous input (ARX) model. To estimate the hidden centers, the radial basis function widths and the connection weights of the RBFNN, a new gradient descent algorithm is derived in the study. On the other hand, the least squares (LS) algorithm and Akaike Information Criteria (AIC) are used to estimate the parameters and the orders of the ARX model, respectively. The applicability of the proposed Hammerstein model in modeling the nonlinear dynamic properties of the SOFC is illustrated by the simulation. At the same time, the experimental comparisons between the Hammerstein model and the RBFNN model are provided which show a substantially better performance for the Hammerstein model. Furthermore, based on this Hammerstein model, some control schemes such as predictive control, robust control can be developed.

Keywords: Solid oxide fuel cell (SOFC); Hammerstein model; Radial basis function neural network (RBFNN); Autoregressive with exogenous input (ARX); Dynamic modeling

1. Introduction

Fuel cell (FC) is considered one of the most important distributed resources due to its modularity, high efficiency and low environmental pollution. The solid oxide fuel cell (SOFC), in particular, can achieve efficiency at least 50% [1]. It presents an attractive option for the distributed generation (DG) technology, which generates electricity at or near the load site.

It is well known that SOFC systems are sealed, and work in a high-temperature (600–1000 °C) environment. As a kind of nonlinear multi-input–multi-output (MIMO) system, SOFC is hard to model by the traditional methodologies. Although there have been many investigations into all aspects of mathematical modeling of the SOFC, most of them are concerned with static performance [2–4]. The SOFC, however, is a dynamic device which will affect the dynamic behavior of the power system to which it is connected. Analysis of such a behavior requires an accurate dynamic model. In the last several decades, fruitful results on modeling the nonlinear dynamics of the SOFC have been proposed [5–8]. However, most of these models emphasized the detailed description of cell internal processes, such as component material balance, energy balance and electrochemical kinetics, etc. These models are very useful for analyzing the transient characteristics of the SOFC, but they are too complicated to be used in a control system design. To develop effective control strategies, an autoregressive with exogenous input (ARX) identification model for a SOFC has been presented in Ref. [9]. However, the performance of this model may be poor due to the highly nonlinear behavior of the system. Therefore, a new nonlinear modeling approach is needed to provide a better solution. In this work, a Hammerstein model, consisting of a radial basis function neural network (RBFNN) in cascade with an ARX model, is adopted to describe the nonlinear dynamic properties of the SOFC.

∗ Corresponding author. Tel.: +86 21 62932154; fax: +86 21 62932154.
E-mail address: huohb1028@sjtu.edu.cn (H.-B. Huo).

0378-7753/$ – see front matter © 2007 Elsevier B.V. All rights reserved.
doi:10.1016/j.jpowsour.2007.09.059

Nomenclature

E_0	ideal standard potential (V)
E	open-circuit reversible potential (V)
F	Faraday's constant (96487 C mol^{-1})
I_{FC}	stack current (A)
K_i	valve molar constants for hydrogen, oxygen and water (mol s^{-1} atm^{-1})
K_r	constant with the value of $N_0/4F$ (mol s^{-1} A^{-1})
$N_{H_2}^{out}$	hydrogen output flow rate (mol s^{-1})
$N_{H_2}^{in}$	hydrogen input flow rate (mol s^{-1})
$N_{H_2}^{r}$	hydrogen reacted flow rate (mol s^{-1})
$N_{O_2}^{in}$	oxygen input flow rate (mol s^{-1})
N_f	natural gas input flow (mol s^{-1})
N_0	number of cells in the stack
p_i	partial pressures of hydrogen, oxygen, and water (atm)
R	gas constant (8.31 J mol^{-1} K^{-1})
r	ohmic loss (Ω)
r_{H_O}	ratio of hydrogen to oxygen
T	stack operating temperature (K)
u	fuel utilization
u_s	desired utilization in steady-state
V_{dc}	stack output voltage (V)

Greek letter

τ_f	fuel processor response time (s)
τ_i	response times for the flow of hydrogen, oxygen and water (s)
η	learning rate

The Hammerstein model consists of a static nonlinear part followed in series by a dynamic linear part. It is a type of commonly used nonlinear model, and has been successfully used to model a class of nonlinear systems [10–13]. The identification of the Hammerstein system involves estimating both the nonlinear and the linear parts from the input–output observations. In Ref. [14], Jurado has presented a Hammerstein model for SOFC, in which the base functions were used for the representation of the linear and nonlinear blocks in the Hammerstein model. But this kind of identification method needs prior information of the system [15]. To overcome the aforementioned deficiencies, Narendra and Parthasarathy [16] have pointed out that a neural network could be used as the nonlinear operator in a Hammerstein model. Due to a number of advantages of RBFNNs compared with other types of artificial neural networks (ANNs), such as better approximation properties, simpler network structures and faster learning algorithms [17], a Hammerstein model of the SOFC is presented in this study, in which the nonlinear static part is approximated by a RBFNN and the linear dynamic part is modeled by an ARX model.

In addition, one of the most important cell performance variables, fuel utilization, has not been examined in Ref. [14] when they explored the SOFC dynamic response after the disturbances. Furthermore, they have not included the SOFC fuel processor in their investigation. So in this paper, the fuel processor is included and the operating issue about the fuel utilization is considered specifically.

The rest of this paper is organized as follows. In Section 2, the SOFC dynamic model proposed in Refs. [8,18,19] is briefly reviewed. The identification structure and identification algorithms of the Hammerstein model are given in Section 3. In Section 4, the detailed identification process of the Hammerstein model for the SOFC is described and some simulation results are given. Finally, conclusions are presented in Section 5.

2. Theory for the SOFC dynamic model

Based on the work reported in Refs. [8,18,19], the SOFC dynamic model is briefly reviewed in this section. The SOFC dynamic model including the fuel processor adopted in this paper is shown in Fig. 1 [18].

2.1. The balance of plant (BOP)

The BOP consists of the natural gas fuel storage, fuel valve controlled by its controller, and the fuel processor that reforms the natural gas input N_f to the hydrogen-rich fuel $N_{H_2}^{in}$. In Ref. [8], the authors introduced a simple model of a fuel processor that converts fuels such as natural gas to hydrogen and byproduct gases. The model is a first-order transfer function with time constant τ_f. Hence, the fuel processor is represented simply by this first-order model.

Although CO can be a fuel in a SOFC, we suppose all CO will take part in the CO-shift reaction if the gas contains water [8]. Thus, the overall cell reaction of the SOFC is:

$$H_2 + \frac{1}{2}O_2 \rightarrow H_2O \quad (1)$$

From Eq. (1), it is seen that the stoichiometric ratio between hydrogen and oxygen is 2 to 1. Oxygen excess is always taken in to let hydrogen react with oxygen more completely. So, the flow ratio of hydrogen to oxygen is kept at 1.145 in this paper [18].

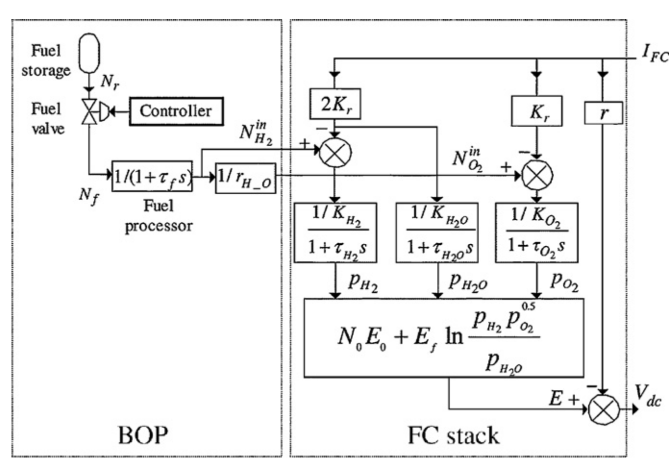

Fig. 1. SOFC dynamic model.

2.2. Solid oxide fuel cell

The SOFC consists of hundreds of cells connected in series or in parallel. By regulating the fuel valve, the amount of fuel into the SOFC stack can be adjusted, and the output voltage of the SOFC can be controlled.

The Nernst's equation and Ohm's law determine the average voltage magnitude of the fuel cell stack. So, applying Nernst's equation and Ohm's law (taking into account ohmic losses), the output voltage of the SOFC can be modeled as follows [5,8,18,19]:

$$V_{\mathrm{dc}} = E - rI_{\mathrm{FC}} \tag{2}$$

$$E = N_0 E_0 + \frac{N_0 RT}{2F} \ln \frac{p_{\mathrm{H_2}} p_{\mathrm{O_2}}^{0.5}}{p_{\mathrm{H_2O}}} \tag{3}$$

where

$$p_{\mathrm{H_2}} = \frac{1/K_{\mathrm{H_2}}}{1+\tau_{\mathrm{H_2}} s}(N_{\mathrm{H_2}}^{\mathrm{in}} - 2K_r I_{\mathrm{FC}}) \tag{4}$$

$$p_{\mathrm{O_2}} = \frac{1/K_{\mathrm{O_2}}}{1+\tau_{\mathrm{O_2}} s}(N_{\mathrm{O_2}}^{\mathrm{in}} - K_r I_{\mathrm{FC}}) \tag{5}$$

$$p_{\mathrm{H_2O}} = \frac{1/K_{\mathrm{H_2O}}}{1+\tau_{\mathrm{H_2O}} s} 2K_r I_{\mathrm{FC}} \tag{6}$$

2.3. Fuel utilization

Fuel utilization is one of the most important operating variables that may affect the performance of FC. It is defined as:

$$u = \frac{N_{\mathrm{H_2}}^{\mathrm{in}} - N_{\mathrm{H_2}}^{\mathrm{out}}}{N_{\mathrm{H_2}}^{\mathrm{in}}} = \frac{N_{\mathrm{H_2}}^{\mathrm{r}}}{N_{\mathrm{H_2}}^{\mathrm{in}}} = \frac{N_0 I_{\mathrm{FC}}}{2FN_{\mathrm{H_2}}^{\mathrm{in}}} \tag{7}$$

where $N_{\mathrm{H_2}}^{\mathrm{r}}$ is the hydrogen reacted flow rate. For protecting the SOFC stack, the desired range of fuel utilization is from 0.7 to 0.9. An overused-fuel condition ($u > 0.9$) could lead to permanent damage to the cells due to fuel starvation whereas an underused-fuel condition ($u < 0.7$) results in a rapid rise of the cell voltage [20].

To protect the SOFC stack and expect small deviations in the terminal voltage due to changes in stack current, we will hold the utilization as constant. According to Eq. (7), the operation of the SOFC stack with a fuel input proportional to the stack current results in a constant utilization factor in the steady-state. Thus, the SOFC stack is operated with constant steady-state utilization by controlling the natural gas input flow to the stack as [19]:

$$N_{\mathrm{f}} = \frac{N_0 I_{\mathrm{FC}}}{2Fu_{\mathrm{s}}} \tag{8}$$

where u_{s} is the desired utilization in steady-state. Furthermore, because the fuel processor is specially considered, the relationship between a small change of stack current ΔI_{FC} and a small change of hydrogen input $\Delta N_{\mathrm{H_2}}^{\mathrm{in}}$ fed to the SOFC stack can be derived as [19]:

$$\Delta N_{\mathrm{H_2}}^{\mathrm{in}} = \frac{N_0}{2Fu_{\mathrm{s}}(1+\tau_{\mathrm{f}} s)} \Delta I_{\mathrm{FC}} \tag{9}$$

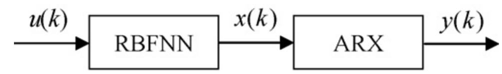

Fig. 2. Hammerstein model.

3. Hammerstein model

3.1. Problem statement

In this section, we will consider the problem of estimating a model for a single-input–single-output (SISO) Hammerstein system based on the input–output data, i.e., $\{u_i\}_{i=1,\ldots,n}$ and $\{y_i\}_{i=1,\ldots,n}$. The Hammerstein model consists of a RBFNN for identification of the static nonlinear part, in series with an ARX model for identification of the linear part. The structure of the Hammerstein model adopted in this paper is illustrated in Fig. 2, where $u(k)$ and $y(k)$ are the input and output of the Hammerstein model at the kth sampling instant, respectively, and $x(k)$ is the output of RBFNN which is unmeasurable. The output of the Hammerstein model can be expressed as:

$$y(k) = -\sum_{i=1}^{n_a} a_i y(k-i) + \sum_{j=0}^{n_b} b_j x(k-j) \tag{10}$$

where $a_i (i = 1, \ldots, n_a)$ and $b_j (j = 0, \ldots, n_b)$ are the parameters of the ARX model, n_a and n_b are integers related to the model order and the function.

The static nonlinear part in the Hammerstein model is represented by using the RBFNN depicted in Fig. 3 as:

$$x(k) = \sum_{i=1}^{M} w_i \phi_i(u(k)) \tag{11}$$

where

$$\phi_i(u(k)) = \exp\left(-\frac{||u(k) - c_i||^2}{2d_i^2}\right) \tag{12}$$

is the Gaussian function. M is the number of hidden node, c_i and d_i are the centers and widths of the ith RBF hidden unit, respectively. w_i is the connection weight from the ith hidden node to the output, $||\cdot||$ denotes the Euclidean norm.

3.2. Identification of the Hammerstein model

The identification of the Hammerstein model involves estimating the hidden centers, the radial basis function widths and the connection weights of the RBFNN and the orders and parameters of the ARX model. The objective is to develop training algorithms by which we can adjust the above parameters so that the application of a set of inputs produces a desired set of outputs.

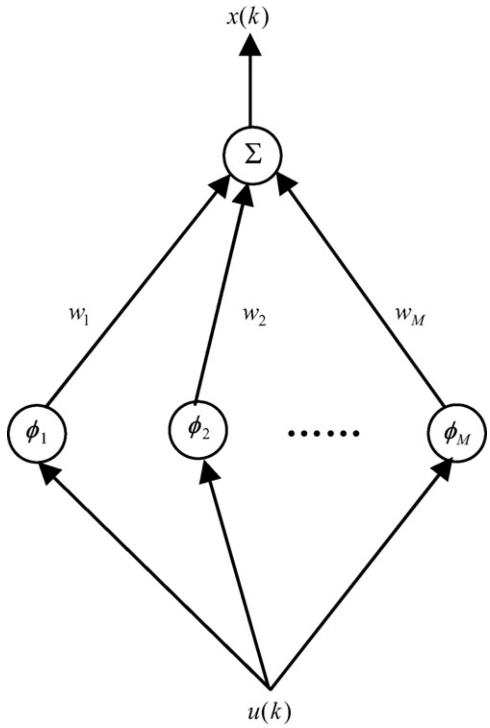

Fig. 3. RBF neural network.

3.2.1. Identification of the RBFNN

For a neural network, gradient-based learning algorithm is commonly used in network training. In this research, a new gradient descent algorithm is derived to update the hidden centers, the radial basis function widths and the connection weights of the RBFNN in the Hammerstein model.

In order to adjust the hidden centers, the radial basis function widths and the connection weights of the RBFNN by using gradient-based learning algorithm, a problem arises in determining a measure of the error at the output of the RBFNN. One knows the desired output ($y(k)$) of the Hammerstein model, but the desired output ($x(k)$) for the RBFNN is unknown in advance. Intuitively, the error at the output of the RBFNN must be related to the error at the output of the ARX model [21]. This idea is used to derive the updating laws for the connection weights, the hidden centers and the radial basis function widths of the RBFNN by defining the following error at the output of the ARX model:

$$E(k) = \tfrac{1}{2}(y_{\rm d}(k) - y(k))^2 \tag{13}$$

where $y_{\rm d}(k)$ is the desired output of the system. Combining Eqs. (10), (11) and (13), one gets

$$\begin{aligned} E(k) &= \frac{1}{2}(y_{\rm d}(k) + a_1 y(k-1) + \cdots + a_{n_a} y(k-n_a) \\ &\quad - b_0 x(k) - \cdots - b_{n_b} x(k-n_b))^2 \\ &= \frac{1}{2}(y_{\rm d}(k) + a_1 y(k-1) + \cdots + a_{n_a} y(k-n_a) \\ &\quad - b_0 \left(\sum_{i=1}^{M} w_i \phi_i(u(k))\right) - \cdots - b_{n_b} x(k-n_b))^2 \end{aligned} \tag{14}$$

To minimize the error $E(k)$, the connection weights w_i, the hidden centers c_i and the radial basis function widths d_i should be updated in the negative direction of the gradient of $E(k)$, $\nabla E(k)$. Thus, the updating laws of w_i, c_i and d_i are derived as follows:

$$\nabla w_i(k) = -\eta \frac{\partial E(k)}{\partial w_i(k)} = b_0 \eta (y_{\rm d}(k) - y(k)) \phi_i(u(k)) \tag{15}$$

$$w_i(k+1) = w_i(k) + b_0 \eta (y_{\rm d}(k) - y(k)) \phi_i(u(k)) \tag{16}$$

$$\begin{aligned} \nabla c_i(k) &= -\eta \frac{\partial E(k)}{\partial c_i(k)} \\ &= b_0 \eta w_i(k)(y_{\rm d}(k) - y(k)) \phi_i(u(k)) \frac{u(k) - c_i(k)}{(d_i(k))^2} \end{aligned} \tag{17}$$

$$\begin{aligned} c_i(k+1) &= c_i(k) + b_0 \eta w_i(k)(y_{\rm d}(k) \\ &\quad - y(k)) \phi_i(u(k)) \frac{u(k) - c_i(k)}{(d_i(k))^2} \end{aligned} \tag{18}$$

$$\begin{aligned} \nabla d_i(k) &= -\eta \frac{\partial E(k)}{\partial d_i(k)} = b_0 \eta w_i(k)(y_{\rm d}(k) \\ &\quad - y(k)) \phi_i(u(k)) \frac{||u(k) - c_i(k)||^2}{(d_i(k))^3} \end{aligned} \tag{19}$$

$$\begin{aligned} d_i(k+1) &= d_i(k) + b_0 \eta w_i(k)(y_{\rm d}(k) \\ &\quad - y(k)) \phi_i(u(k)) \frac{||u(k) - c_i(k)||^2}{(d_i(k))^3} \end{aligned} \tag{20}$$

where η is the learning rate.

3.2.2. Identification of the ARX model

An important step, which precedes the parameter estimation of the ARX model, is to determine the model structure which is entirely defined by the integers n_a and n_b. Many statistical model selection criteria have been developed. One popular criterion is the Akaike Information Criterion (AIC) [22]. So in this study, the best orders of the ARX model are determined by minimizing AIC, which is defined as:

$$\text{AIC} = -N \log(E) + 2(n_a + n_b) \tag{21}$$

$$E = \frac{1}{N} \sum_{k=1}^{N} (y(k) - \hat{y}(k))^2 \tag{22}$$

where $\hat{y}(k)$ is the estimated output at time step "k" of the ARX model, N is the number of sample points, E is the mean square error between actual output and estimated output of the ARX model.

In the sequel, the least squares (LS) algorithm is adopted to estimate the parameters of the ARX model, i.e.,

$$\hat{\theta} = [H^{\rm T} H]^{-1} H^{\rm T} Y \tag{23}$$

Table 1
SOFC operating point data

Item	Value
N_0	384
T	1273 K
$I_{FC, rate}$	300 A
u_s	0.8
E_0	1.18 V
K_{H_2}	0.843 mol s^{-1} atm^{-1}
K_{O_2}	2.52 mol s^{-1} atm^{-1}
K_{H_2O}	0.281 mol s^{-1} atm^{-1}
τ_{H_2}	26.1 s
τ_{O_2}	2.91 s
τ_{H_2O}	78.3 s
τ_f	5 s
r	0.126 Ω
r_{H_O}	1.145

where $\hat{\theta} = [\hat{a}_1, \hat{a}_2, \ldots, \hat{a}_{n_a}, \hat{b}_0, \hat{b}_1, \ldots, \hat{b}_{n_b}]^{\mathrm{T}}$ is the estimated parameters of the ARX model and

$$H = [h(1), h(2), \ldots, h(N)]^{\mathrm{T}}_{N\times(n_a+n_b+1)} \tag{24}$$

$$Y = [y(1), y(2), \ldots, y(N)]^{\mathrm{T}}_{N\times 1} \tag{25}$$

$$h(k) = [-y(k-1), -y(k-2), \ldots, -y(k-n_a), (k), (k-1), \ldots, (k-n_b)]^{\mathrm{T}}_{(n_a+n_b+1)\times 1} \tag{26}$$

4. Results and discussion

The main aim of this paper is to construct a dynamic model for the output voltage V_{dc} of the SOFC, as a function of the natural gas input flow to the stack N_f. For the purpose of identification, the white-box model described in Section 2 is used to generate the modeling data. In the following condition, it is assumed that the load resistor has the following variation. The SOFC is operating at its rated operation point initially. The nominal operating conditions of the SOFC are given in Table 1 [8,18]. At $t = 150$ s, a load disturbance causes the stack current to have a step change (from 300 to 270 A). In this situation, the variation of the natural gas input flow to the stack is depicted in Fig. 4. In order to establish the Hammerstein model, a record of 600 experimental samples of the output voltage is collected due to this change of the natural gas input flow.

Based on these data, we firstly determine the structure of the ARX model in the Hammerstein model. To determine the orders of the ARX model, the sampled input–output data are used to identify a linear ARX model for the SOFC [14]. By minimizing AIC, the structure of the ARX model can be determined as follows:

$$\begin{aligned} V_{dc}(k) = &-a_1 V_{dc}(k-1) - a_2 V_{dc}(k-2) - a_3 V_{dc}(k-3) \\ &-a_4 V_{dc}(k-4) - a_5 V_{dc}(k-5) - a_6 V_{dc}(k-6) \\ &-a_7 V_{dc}(k-7) - a_8 V_{dc}(k-8) - a_9 V_{dc}(k-9) \\ &+b_0 x(k) + b_1 x(k-1) + b_2 x(k-2) + b_3 x(k-3) \\ &+b_4 x(k-4) + b_5 x(k-5) + b_6 x(k-6) \end{aligned} \tag{27}$$

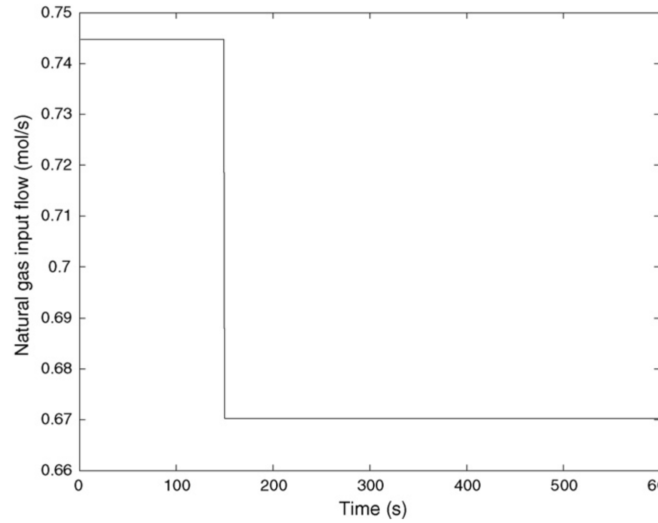

Fig. 4. Variation of the natural gas input flow due to step change of current from 300 to 270 A.

Thus, the structure of the Hammerstein model selected in this paper will consist of a RBFNN with six RBF neurons in the hidden layer as shown in Fig. 3, and an ARX model with the structure as shown in Eq. (27).

Secondly, the connection weights w_i, the hidden centers c_i and the radial basis function widths d_i of the RBFNN are initialized with small random values. Thus, one can convert the natural gas input flow, $N_f(k)$, into the intermediate variable, $x(k)$, using Eq. (11). After selecting the learning rate $\eta = 0.004$, the LS algorithm (i.e., Eq. (23)) and the derived gradient descent learning algorithm (i.e., Eqs. (15–20)) are used to adjust the parameters of the ARX model and the RBFNN, respectively. As a result, the actual output voltage of the SOFC and the identified output voltage of the Hammerstein model are shown in Fig. 5. Fig. 5 indicates that the proposed Hammerstein modeling method is applicable to describe the nonlinear dynamic behaviors of the SOFC.

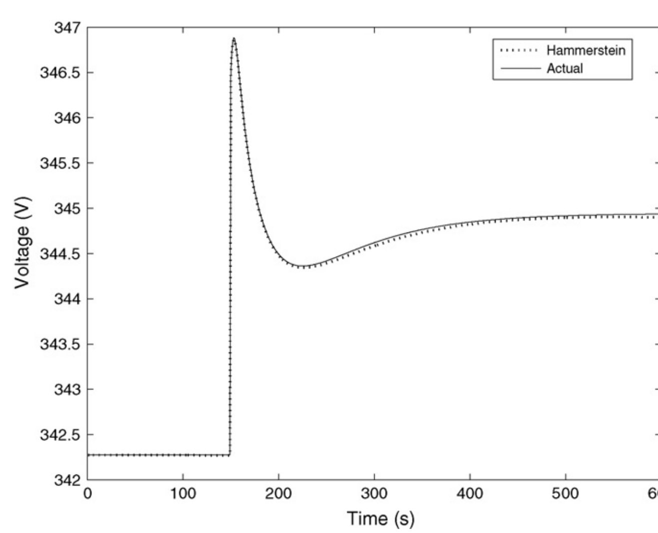

Fig. 5. Output voltage of the actual and identified Hammerstein models.

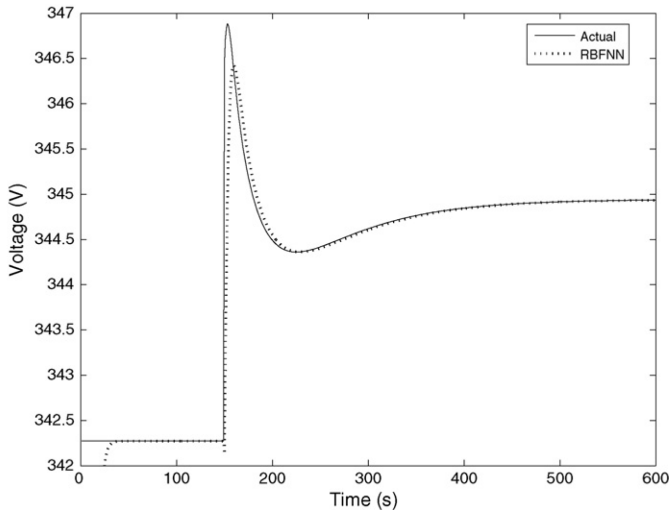

Fig. 6. Output voltage of the actual and identified RBFNN models.

For the purpose of comparison, the same input–output data are used to identify a RBFNN model, which performs at the same structure and initial values of the RBFNN parameters as in the Hammerstein model. In this study, the traditional gradient descent algorithm is used to adjust the RBFNN parameters. Finally, the actual output voltage of the SOFC and the estimated output voltage of the RBFNN model are depicted in Fig. 6. Comparing the identification results in Figs. 5 and 6, one will notice that the Hammerstein model yields higher modeling accuracy. These indicate the Hammerstein model is a powerful tool for describing the nonlinear dynamic properties of the SOFC and the Hammerstein model presented is accurate and valid.

5. Conclusions

To develop control schemes, a nonlinear modeling study of the SOFC using a Hammerstein model is reported in this paper. The Hammerstein model consists of a RBFNN in series with an ARX model. To estimate the connection weights, the hidden centers and the radial basis function widths of the RBFNN, a new gradient descent algorithm is derived. On the other hand, the AIC and the standard LS algorithm are used to determine the orders and the parameters of the ARX model, respectively.

Besides, the performance of our proposed Hammerstein model has been tested and compared with the RBFNN model. Simulation results show that the Hammerstein model yields higher modeling accuracy. These indicate that it is feasible to establish the Hammerstein model for describing the nonlinear dynamic properties of the SOFC, and the Hammerstein model presented in this paper is accurate and valid. In the future, based on this Hammerstein model, some control schemes such as predictive control and robust control can be developed.

Acknowledgment

This work is supported by National 863 Scientific Project Development Funds (No. 2006AA05Z148), PR China.

References

[1] P. Costamagna, L. Magistri, A.F. Massardo, J. Power Sources 96 (2) (2001) 352–368.
[2] J. Arriagada, P. Olausson, A. Selimovic, J. Power Sources 112 (1) (2002) 54–60.
[3] P. Aguiar, C.S. Adjiman, N.P. Brandon, J. Power Sources 138 (2004) 120–136.
[4] H.B. Huo, X.J. Zhu, G.Y. Cao, J. Power Sources 162 (2) (2006) 1220–1225.
[5] J. Padulles, G.W. Ault, J.R. McDonald, J. Power Sources 86 (1–2) (2000) 495–500.
[6] D.J. Hall, R.G. Colclaser, IEEE Trans. Energy Convers. 14 (3) (1999) 749–753.
[7] K. Sedghisigarchi, A. Feliachi, IEEE Trans. Energy Convers. 19 (2) (2004) 423–428.
[8] Y. Zhu, K. Tomsovic, Elect. Power Syst. Res. 62 (1) (2002) 1–11.
[9] F. Jurado, J. Power Sources 129 (2) (2004) 205–215.
[10] R.K. Pearson, M. Pottmann, J. Process Control 10 (4) (2000) 301–315.
[11] H.T. Su, T.J. McAvoy, Ind. Eng. Chem. Res. 26 (1993) 1927–1936.
[12] D.K. Rollins, N. Bhandari, A.M. Bassily, G.M. Colver, S.T. Chin, Ind. Eng. Chem. Res. 42 (4) (2003) 860–872.
[13] A. Balestrino, A. Landi, M. Ould-Zmirli, L. Sani, IEEE Trans. Ind. Electron. 48 (3) (2001) 645–655.
[14] F. Jurado, J. Power Sources 154 (1) (2006) 145–152.
[15] L.M. Sun, W.J. Liu, A. Sano, Proceedings of the 1996 UKACC International Conference on Control, Exeter, UK, 1996, pp. 240–245.
[16] K.S. Narendra, K. Parthasarathy, IEEE Trans. Neural Netw. 1 (1) (1990) 4–27.
[17] H. Sarimveis, A. Alexandridis, S. Mazarakis, G. Bafas, Comput. Chem. Eng. 28 (1–2) (2004) 209–217.
[18] Y.H. Li, S.S. Choi, S. Rajakaruna, IEEE Trans. Energy Convers. 20 (2) (2005) 381–387.
[19] Y.H. Li, S. Rajakaruna, S.S. Choi, IEEE Trans. Energy Convers. 22 (2) (2007) 405–413.
[20] K. Sedghisigarchi, A. Feliachi, IEEE Trans. Energy Convers. 21 (1) (2006) 250–256.
[21] H. Al-Duwaish, M.N. Karim, Automatica 33 (10) (1997) 1871–1875.
[22] L. Ljung, System Identification: Theory for the User, second ed., Prentice Hall, Englewood Cliffs, NJ, 1999.